

PTPN2 improves implant osseointegration in T2DM via inducing the dephosphorylation of ERK

Ya-Nan Wang^{1,2,3}, Tingting Jia^{1,2,3}, Jiajia Zhang^{1,2,3}, Jing Lan^{1,2,3}, Dongjiao Zhang^{1,2,3}  and Xin Xu^{1,2,3}

¹Department of Implantology, School and Hospital of Stomatology, Shandong University, Shandong 250012, China; ²Shandong Provincial Key Laboratory of Oral Tissue Regeneration, Shandong 250012, China; ³Shandong Engineering Laboratory for Dental Materials and Oral Tissue Regeneration, Shandong 250012, China

Corresponding authors: Dongjiao Zhang. Email: djzhang1109@163.com; Xin Xu. Email: xinxu@sdu.edu.cn

Impact statement

Using both *in vivo* and *in vitro* approaches, we made important findings that PTPN2 promoted implant osseointegration in T2DM rats and enhanced osteogenesis of RBMSCs in high glucose medium. The positive effects of PTPN2 on osteogenesis are related to the dephosphorylation of ERK and the inhibition of MAPK/ERK pathway. PTPN2 may be a novel target for the therapy of impaired implant osseointegration in T2DM patients.

Abstract

Type 2 diabetes mellitus (T2DM) is considered to compromise implant osseointegration. Protein tyrosine phosphatase non-receptor type 2 (PTPN2) regulates glucose metabolism, systemic inflammation, and bone regeneration. This study aimed to investigate the role of PTPN2 in implant osseointegration in T2DM and explore the potential mechanisms. Streptozotocin-induced diabetic rats received implant surgery, with or without local overexpression of PTPN2 for three months, and implant osseointegration was examined by histological evaluation, micro-CT analysis, pull-out test, and scanning electron microscope. Rat bone marrow stem cells (RBMSCs) were isolated and exposed to high glucose, and

osteogenic differentiation was evaluated by alizarin red staining, ALP assay, and Western blot analysis. Overexpression of PTPN2 could improve impaired implant osseointegration in T2DM rats and promote osteogenic differentiation of RBMSCs in high glucose. In addition, p-ERK level in RBMSCs was increased in high glucose and decreased after PTPN2 overexpression. These results suggest that PTPN2 promotes implant osseointegration in T2DM rats and enhances osteogenesis of RBMSCs in high glucose medium via inducing the dephosphorylation of ERK. PTPN2 may be a novel target for the therapy of impaired implant osseointegration in T2DM patients.

Keywords: Type 2 diabetes mellitus, osseointegration, PTPN2, MAPK signaling, ERK

Experimental Biology and Medicine 2019; 244: 1493–1503. DOI: 10.1177/1535370219883419

Introduction

Type 2 diabetes mellitus (T2DM) is a prevalent metabolic disease characterized by hyperglycemia and it impairs the process of implant osseointegration.¹ The negative effects of T2DM on implant osseointegration may be associated with inflammatory reactions, impaired osteoblast differentiation, and reduction of bone turnover,² but the detailed mechanisms are still unclear. Over the past decade, many strategies such as pharmacological agents and implant surface modifications attempted to increase osseointegration of implants in T2DM, but few of them are available as a routine treatment method in clinical settings.^{3–5} Therefore,

it is urgent to develop new treatment strategies to improve the osseointegration of implants in T2DM patients.

Protein tyrosine phosphatase non-receptor type 2 (PTPN2), also known as T cell protein tyrosine phosphatase (TCPTP), is a tyrosine-specific phosphatase ubiquitously expressed in various cells in the human body.⁶ Accumulating evidence has indicated that PTPN2 plays an important role in glucose metabolism.⁷ PTPN2 could attenuate signal transducer and activator of transcription-3 (STAT3) and insulin signaling in the liver to regulate gluconeogenesis.⁸ PTPN2 overexpression in epididymal white adipose tissue could inhibit systemic inflammation via

T cells polarization shift in diabetic mice.⁹ In addition, PTPN2 regulates bone resorption and whole-body insulin sensitivity.¹⁰ However, the effect of PTPN2 on implant osseointegration in hyperglycemia and the potential mechanisms is unclear.

Mitogen-activated protein kinase (MAPK) signaling pathway plays a critical role in a variety of cellular activities.¹¹ There are three major MAPKs in mammalian cells, namely extracellular signal-regulated kinase (ERK), c-Jun-N-terminal kinase (JNK), and p38 MAPK. Furthermore, hyperglycemia can activate MAPK signaling pathway via inducing the phosphorylation of ERK, p38, and JNK.¹² It should be pointed out that the activation of MAPKs by hyperglycemia has a negative effect of osteogenesis in T2DM.¹³ Therefore, the inhibition of MAPK pathway would be an effective way to improve implant osseointegration. PTPN2 can specifically regulate signaling pathways by dephosphorylating distinct substrates, including MAPK pathway.¹⁴ Therefore, we hypothesized that PTPN2 might promote implant osseointegration in T2DM through inducing the dephosphorylation/inactivation of MAPK signaling pathway. In this study, we examined osseointegration of femoral implant *in vivo* and the osteogenic ability of rat bone marrow stem cells (RBMSCs) *in vitro* to investigate the role of PTPN2 in implant osseointegration in T2DM and explore the potential mechanisms.

Materials and methods

Establishment of T2DM rat model

Twenty-four age-matched male Sprague Dawley rats (weight 200 ± 20 g) were provided by Beijing Vital River Laboratory Animal Technology Co., Ltd (China) and kept in Experimental Animal Center of Shandong University (Jinan, China). All experimental procedures were approved by Animal Ethics Committee of Shandong University (Jinan, China). All animal experiments were carried out in accordance with National Institutes of Health guide for the care and use of Laboratory animals (NIH Publications No. 8023, revised 1978). After one-week acclimation, all rats were randomly divided to control group (N group, $n = 6$) and type 2 diabetic group ($n = 18$). T2DM rats were induced by four-week high-fat and high-carbohydrate diet (Beijing Ke'ao Xieli Feed Co. Ltd, China), followed by intraperitoneal injection with streptozotocin (STZ, Sigma, USA) at a dose of 35 mg/kg in 0.1 M citrate-buffered saline (pH = 4.2) once.¹⁵ The control group received normal chow and citrate buffer injection. Fasting blood glucose (FBG) ≥ 13.9 mmol/L one week after STZ injection was considered to be the standard for successful T2DM rat model.¹⁶ Subsequently, diabetes rats with similar degrees of hyperglycemia were randomly divided into T2DM group ($n = 6$), T2DM+PTPN2 group ($n = 6$), and T2DM+Vehicle group ($n = 6$).

Implant placement

Animals were anesthetized by pentobarbital sodium (40 mg/kg body weight, Sigma, USA). Subsequently, every rat received two special designed sand-blasted and acid-etched (SLA) porous mini-Ti implants (1 mm in diameter

and 10 mm in length, Wego, China) in the distal femora as previously reported.¹⁷ A 10 mm longitudinal incision was made along the medial side of the knee joint, and the patella was dislocated laterally to expose the distal metaphysis of the femur. With the knee in flexion, a 1.0-mm diameter and 10.0-mm long hole was made from the intercondylar notch to the proximal end of femur with surgical stainless steel drills cooled under sterile saline solution. The implant was then inserted into the prepared hole via distal femoral metaphysis until the implant end was below the articular surface which was nearly parallel to the long axis of the femur. The patella was relocated and soft tissues were sutured. The animals received intramuscular injection of penicillin (800,000 IU/ml, Harbin Pharmaceutical Group Co., Ltd, China) for three postoperative days. All rats were euthanized after three months. Five fresh femur samples were used to perform pull-out tests, while others were fixed in 4% polyformaldehyde and preserved in 70% alcohol at 4°C. Fasting blood glucose and body weight were measured every two weeks after implantation.

Local overexpression of PTPN2 in rats

2×10^9 adeno-associated virus (AAV) particles constitutively expressing PTPN2 (Genechem, Shanghai, China) were injected into the knee joint capsule. The control group was injected with the vehicle. The injection was repeated every two weeks till the end of the experiment. The experimental design *in vivo* is shown in Figure 1.

Histological analysis

Histologic samples were dehydrated in a series of graded alcohol solutions and embedded in polymethyl methacrylate (PMMA, Merck AG, Germany). For each sample, the cross section of the implant with 100 μ m thickness was prepared by hard tissue slicer (Leica, Germany). Next, the sections were stained with toluidine blue. The index of bone-implant contact (BIC) was calculated by Image-Pro Plus 6.0 as the length percentage of direct bone-implant interface to total implant circumference.¹⁸

Microscopic computerized tomography analysis

Microscopic computerized tomography (Xradia 510 Versa, Zeiss, Germany) was used to evaluate osseointegration of the implant (60 kV, 5 w, 9.8454 μ m pixel resolution, 3 s exposure time). The region of interest (ROI) was defined as the 200 μ m region around the implant. Bone volume per total volume (BV/TV) and percentage of osseointegration (OI%) were calculated by Mimics software 17.0. BV represents the bone volume in the ROI and TV represents the total space volume of the ROI. OI% is the area proportion of direct bone-implant interface to total implant surface.

Pull-out test

The maximum pull-out force represents the maximum retention force obtained by the implant in the bone. Immediately after collection, five samples of each group were subjected to pull-out test by the universal material

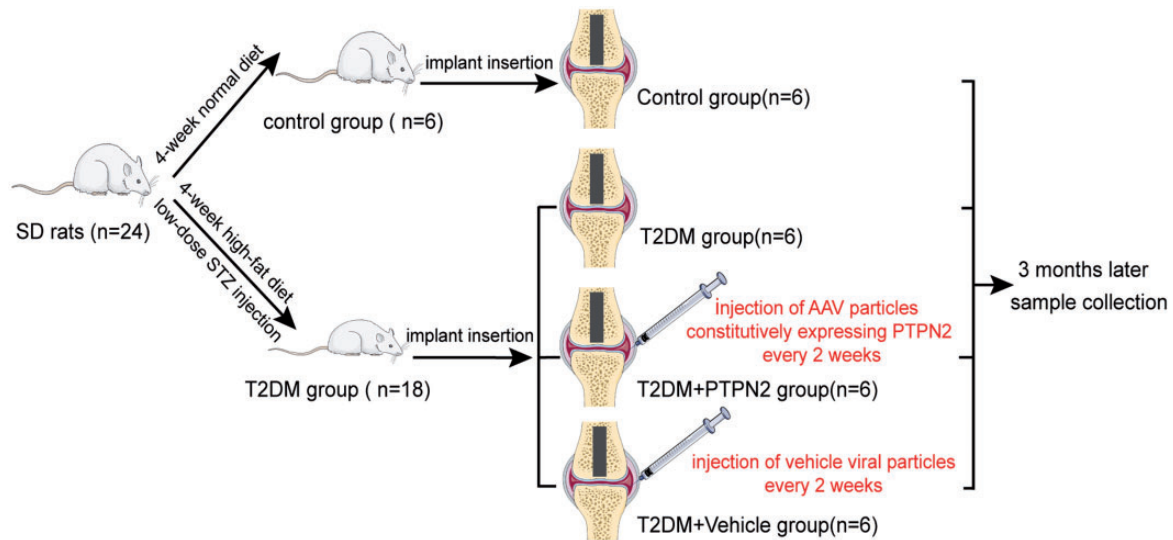


Figure 1. Illustration of the experimental design in vivo. SD rats: Sprague Dawley rats; STZ: streptozotocin; AAV: adeno-associated virus. (A color version of this figure is available in the online journal.)

testing instrument (Shimadzu, Japan) at a constant speed of 1 mm/min until the bone-implant interface ruptured.

Scanning electron microscopy

The surface of SLA porous mini-Ti implant was observed by SEM. After three months healing, implants were pulled out to observe the adhesion and microstructure of the bone on the implant surface under a scanning electron microscope (Inspect F, FEI, Nederland) at an accelerated voltage of 1 kV.

Immunohistochemistry staining

IHC staining was performed on prepared decalcified sections to investigate the expression of PTPN2 (Abcam, ab180764, 1:150 dilution) and ALP (Abcam, ab108337, 1:300 dilution) in peri-implant osseous tissues according to the procedure. For quantitative assessment, five slices of each sample were analyzed in every group by Image J software (National Institutes of Health, Bethesda, MD, USA). The mean integrated optical density (IOD) for PTPN2 and ALP were also calculated.

Cell culture, treatment, transfection, and osteogenic induction

Rat bone marrow stem cells (RBMSCs) were isolated from rat femur bone marrow as reported previously.¹⁹ Cells at the third to fifth passages were used for experiments. Cells were cultured in Dulbecco's modified Eagle's medium (DMEM, Hyclone, USA) supplemented with 10% fetal bovine serum (FBS, Hyclone, USA) at 37°C in a 5% CO₂ incubator. Cells were treated as following groups: (1) normal control group (NC group), cells were cultured in complete culture medium containing 5.5 mmol/L D-glucose; (2) high glucose group (HG group), cells were incubated with complete culture medium containing 30 mmol/L glucose; (3) high glucose with PTPN2 overexpression group (HG+PTPN2 group), cells were infected

with lentivirus constitutively expressing PTPN2 and cultured in complete culture medium with 30 mmol/L glucose²⁰; (4) high glucose with vehicle group (HG+Vehicle group), cells were treated with vehicle and cultured in complete culture medium with 30 mmol/L glucose. For osteogenic induction, RBMSCs were cultured in an osteogenic induction medium containing DMEM supplemented with 10% FBS, 50 mg/L ascorbic acid (Sigma, USA), 10 nM dexamethasone (Solarbio, China), and 10 mM β -glycerophosphate (Solarbio, China).

Alkaline phosphatase assay

After seven days of osteogenic induction, ALP activity was measured by Alkaline Phosphatase Assay Kit (Nanjing Jiancheng Bioengineering Institute, China) according to the manufacturer's instructions. The OD absorbance at 520 nm wavelength was measured by microplate spectrophotometer.

Alizarin red staining

After 28 days of osteogenic induction, cells were fixed in 4% paraformaldehyde for 30 min, rinsed with ddH₂O three times, and stained with 0.1% Alizarin Red (Sigma, USA) at room temperature for 10 min. Next, the mineralized nodule was observed under light microscope (Olympus IX73, Tokyo, Japan). For quantifying the relative amount of calcium, 300 μ L of 10% (w/v) cetylpyridinium chloride (Sigma-Aldrich) and 10 mm sodium phosphate (pH 7.0) solution were added to the stained dishes and the absorbance of extracted dye was determined at 562 nm.

RNA isolation and quantitative real-time PCR

After 28 days of induction, total RNA of RBMSCs with different treatments was extracted with Trizol[®] reagent (TaKaRa Bio Inc., Tokyo, Japan), and 1 μ g RNA was transcribed with reverse transcriptase (TaKaRa Bio Inc.) according to the manufacturer's recommendation. Quantitative

Real-time PCR (qRT-PCR) was performed using 1 μ L of cDNA in a 20 μ L reaction volume with Roche 480 in triplicate. The relative expression level of the housekeeping gene β -Actin was used to normalize gene expression in each sample in different groups. PCR conditions were as follows: hot-start enzyme activation at 95°C for 30 s; 55 cycles of denaturation at 95°C for 5 s, annealing at 60°C for 35 s and extension at 72°C for 1 min; finally at 40°C for 30 s. The sequences of the primers for amplification of rats β -Actin, PTPN2, Runx2, Osx and Ocn were as follows: β -Actin, 5'-GAGACCTTCAACACCCAGCC-3' and 5'-GGCCATCTCTTGCTCGAAGTC-3'; PTPN2, 5'-ATCGA GCGGGAGTTCGA-3' and 5'-TCTGGAAACTTGGCC ACTC-3'; Runx2, 5'-AGTGTGTGTGTCGCCATGAT-3' and 5'-CCACTTGGGGTCTAAGAACG-3'; Osx, 5'-GGA AAGGAGGCACAAAGAAGC-3' and 5'-CCCCTTAGGC ACTAGGAGC-3'; Ocn, 5'-ACCCAGAATTACCTGATCC-3' and 5'-AGACCACCCAGCACAAC-3'; The amount of mRNA was calculated for each sample based on the standard curve using the LightCycler® Software 4.0 (Roche, Basel, Switzerland).

Western blot analysis

Proteins were extracted in RIPA buffer (Solarbio, China) containing 1% PMSF (Solarbio, China) and 1% phosphatase inhibitor (Solarbio, China). The protein concentration was determined by BCA assay kit (Beyotime, China); 20 μ g proteins were separated by 10% SDS-polyacrylamide gels and transferred onto polyvinylidene difluoride (PVDF) membranes. The membranes were blocked with 5% fat-free milk, and incubated overnight at 4°C with primary antibodies against PTPN2 (1:1000, Santa Cruz Biotechnology, USA), Runt-related transcription factor 2 (RUNX2, 1:1000, CST, USA), Osterix (OSX, 1:1000, CST, USA), Osteocalcin (OCN, 1:1000, CST, USA), ERK (1:1000, CST, USA), JNK (1:1000, CST, USA), p38(1:1000, CST, USA), p-ERK (1:1000, CST, USA), p-JNK (1:1000, CST, USA), p-p38 (1:1000, CST, USA), and β -Actin (1:1000, CST, USA). The membranes

were washed three times with TBST and incubated with anti-mouse or anti-rabbit HRP-conjugated secondary antibodies (1:20,000) for 1 h at room temperature. The protein bands were detected by enhanced chemiluminescence under Amersham Imager 600 (Millipore, USA) and the gray values were analyzed by Image J software (National Institutes of Health, Bethesda, MD, USA).

Statistical analysis

All data are presented as the mean \pm standard deviation (SD) of at least three independent experiments. Data normality was assessed by Shapiro-Wilk test. In case of normal distribution, one-way ANOVA combined with S-N-K test were used to analyze group-to-group significant differences in SPSS software (SPSS 20.0). Nonparametric tests were used when the data had no normal distribution. Differences were considered statistically significant for P value < 0.05 .

Results

Local overexpression of PTPN2 did not change fasting blood glucose level and body weight in T2DM rats

All rats survived during the whole experimental period and no infection of the implant was observed. After STZ injection, fasting blood glucose level of T2DM rats increased to over 20 mmol/L and remained at this level for three months (Table 1). Of note, there were no significant differences in fasting blood glucose level between T2DM group, T2DM+PTPN2 group, and T2DM+Vehicle group.

Measurements of body weight are shown in Table 1. The rats in T2DM group showed significant decrease in body weight compared with control group ($P < 0.05$), while no differences were found between T2DM group, T2DM+PTPN2 group, and T2DM+Vehicle group.

Table 1. Effect of PTPN2 local overexpression on body weights and fasting blood glucose levels in experimental rats ($n = 6$ /group).

		Control	T2DM	T2DM+PTPN2	T2DM+Vehicle	
Body weight (g)	0 day	274 \pm 11	290 \pm 10	277 \pm 11	279 \pm 12	
	1 week	294 \pm 13	285 \pm 12	286 \pm 12	285 \pm 16	
	2 weeks	313 \pm 11*	289 \pm 9	299 \pm 9	297 \pm 9	
	4 weeks	343 \pm 9*	274 \pm 11	273 \pm 13	279 \pm 9	
	6 weeks	376 \pm 14*	264 \pm 13	265 \pm 13	268 \pm 13	
	8 weeks	398 \pm 10*	254 \pm 12	254 \pm 12	255 \pm 13	
	10 weeks	431 \pm 5*	245 \pm 9	245 \pm 12	243 \pm 9	
	12 weeks	462 \pm 13*	237 \pm 9	236 \pm 11	234 \pm 9	
	Fasting blood glucose (mmol/L)	0 day	4.5 \pm 0.1	4.6 \pm 0.2	4.5 \pm 0.3	4.6 \pm 0.2
		1 week	4.8 \pm 0.1*	21.7 \pm 2.1	20.4 \pm 1.1	22.2 \pm 2.3
		2 weeks	4.7 \pm 0.1*	25.1 \pm 1.2	25.3 \pm 1.3	25.4 \pm 1.0
		4 weeks	4.7 \pm 0.2*	24.1 \pm 1.4	25.4 \pm 1.0	26.0 \pm 0.6
6 weeks		4.6 \pm 0.1*	23.8 \pm 1.1	24.1 \pm 1.1	24.1 \pm 1.3	
8 weeks		4.6 \pm 0.2*	25.7 \pm 0.8	25.2 \pm 1.0	25.9 \pm 1.5	
10 weeks		4.6 \pm 0.2*	25.0 \pm 0.9	25.7 \pm 1.3	25.4 \pm 1.2	
12 weeks		4.6 \pm 0.2*	25.7 \pm 1.5	25.4 \pm 1.2	25.7 \pm 1.2	

Note: 0 day represented the day before STZ induction. 1 week represented the day after STZ injection. 2–12 weeks represented the corresponding time after implantation.

Data were presented as mean \pm SD, * $P < 0.05$, Control group vs. other three groups.

PTPN2 improved implant osseointegration in T2DM rats

Toluidine blue staining showed that the peri-implant bone mass was decreased and scattered in T2DM group. Local overexpression of PTPN2 increased bone mass and density around the implant in T2DM rats (Figure 2(a)). As shown in Figure 2(d), the BIC of T2DM group was significantly decreased compared with control group. Moreover, the contact ratio restored to almost normal level after PTPN2 local overexpression. Approximately 15% more BIC rate was found in implants with PTPN2 overexpression than in vehicle group.

Next, Micro-CT analysis was performed to examine the peri-implant trabecular microstructures (Figure 2(b), (c), (e), and (f)). The red rectangle region in Figure 2(c) showed the 3D reconstruction area. The red circle in Figure 2(b) and the blue rectangle region in Figure 2(c)

showed the region of interest to evaluated osseointegration. In the control group, the implant was almost fully covered by trabecular, but there were relatively few trabecular microstructures around the titanium implant in T2DM group. Local overexpression of PTPN2 could ameliorate the injuries of trabecular significantly. Furthermore, the OI% for T2DM and control group were $24.78 \pm 0.87\%$ and $52.17 \pm 1.27\%$, respectively, and the OI% was significantly higher in T2DM+PTPN2 group than in T2DM+vehicle group. The qualitative analysis of BV/TV showed the same tendency among the four groups (Figure 2(f)).

The biomechanical properties were detected by pull-out test. As shown in Figure 3, the maximum forces decreased in T2DM model, but we observed significant increase of maximum forces in T2DM+PTPN2 group (45.04 ± 1.26 N) compared to T2DM+vehicle group (36.56 ± 0.81 N).

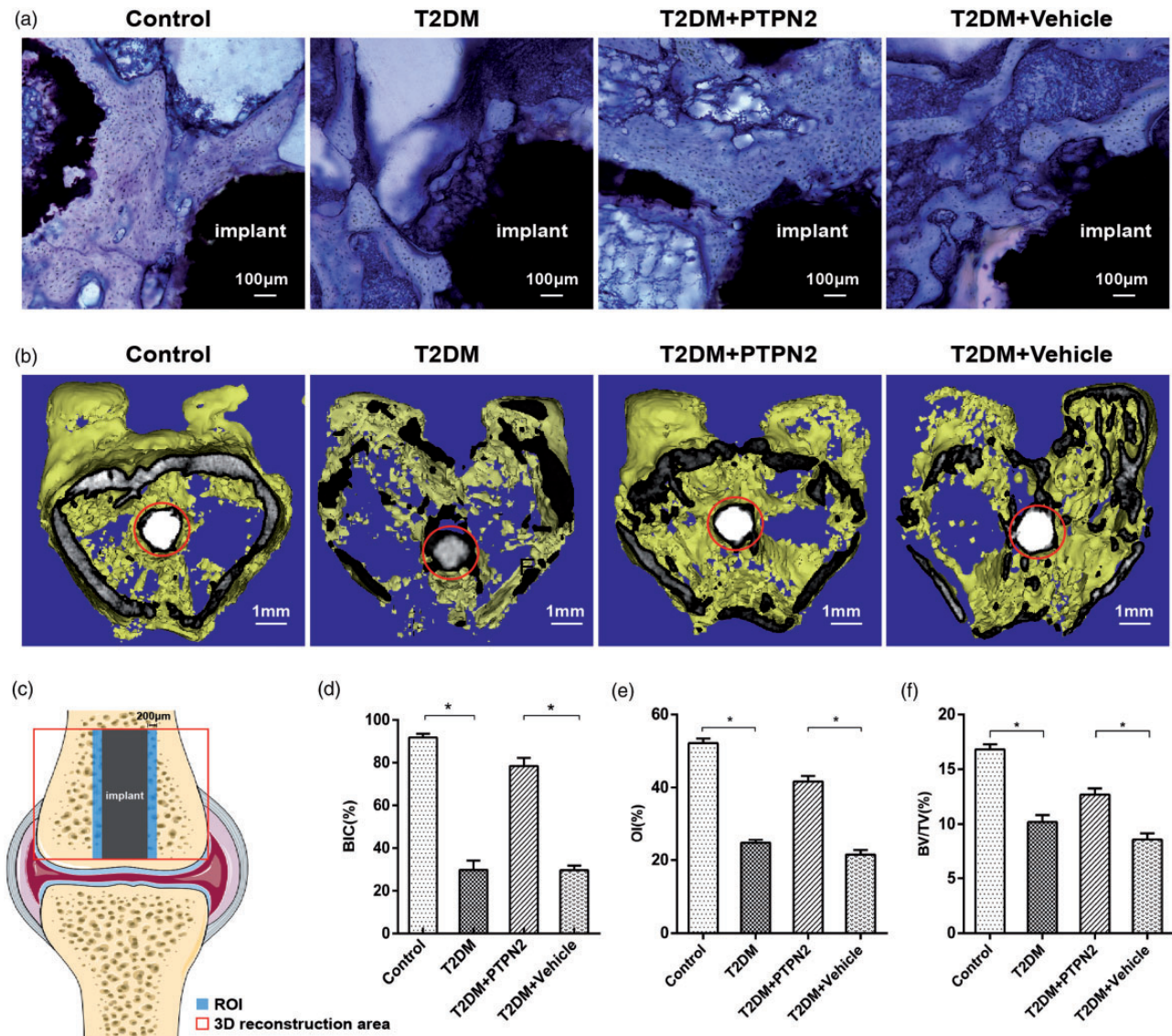


Figure 2. Evaluation of the implant osseointegration after three-month healing. (a) Histological evaluation with toluidine blue staining showed bone microarchitecture at bone-implant interface. (b) Osteogenesis of implants was analyzed by micro-computed tomography three months after surgery. (c) The red rectangle region showed the 3D reconstruction area and the blue rectangle region showed the region of interest to evaluated osseointegration. (d) Bone-implant contact ratio (BIC, %). Quantitative calculation of (e) OI% and (f) BV/TV. Data were presented as mean \pm SD, $n = 5$ specimens/group, * $P < 0.05$. (A color version of this figure is available in the online journal.)

In addition, the microstructure of SLA porous mini-Ti implant and peri-implant bone was analyzed by SEM. The surface of implant was almost occupied by well-organized trabecular pores in control group after three-month healing. In T2DM group, the bone mass was reduced and the porosity of the trabecular bone was increased. However, T2DM+PTPN2 group showed a better bone regeneration not only in bone mass but also in bone density than T2DM+vehicle group (Figure 4). Taken together, the above data indicate that PTPN2 could improve implant osseointegration in T2DM rats.

What's more, immunohistochemistry staining was complete to confirm whether PTPN2 protein was actually overexpressed and detect the expression of the osteogenic marker ALP protein around the implant. Figure 5(a) and (c) indicated PTPN2 and ALP expression in the different groups. Similar to previous results, T2DM rats showed

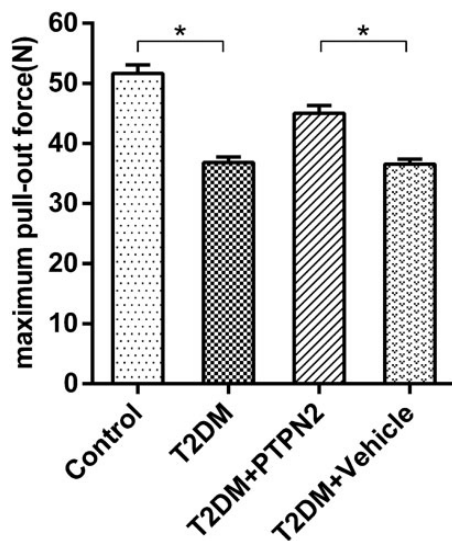


Figure 3 Results of pull-out test three months after implantation. Data were presented as mean \pm SD, $n = 5$ specimens/group, * $P < 0.05$.

lower PTPN2 and ALP concentrations compared to normal rats. And PTPN2 was surely overexpressed in T2DM+PTPN2 group compared to that in vehicle group. Consistent with PTPN2 protein, ALP expression was obviously increased in T2DM+PTPN2 group. The value of IOD/area (Figure 5(b) and (d)) further illustrated that overexpression of PTPN2 can increase the expression of ALP around the implant in T2DM rats.

PTPN2 promoted osteogenic differentiation of RBMSCs exposed to high glucose

To further confirm the role of PTPN2 in implant osseointegration, we established RBMSCs exposed to high glucose (HG) as the model. After 28 days of culture, we found fewer and smaller mineralized nodules in HG group compared with NC group, but cells in HG+PTPN2 group showed similar nodules in size and number compared with NC group (Figure 6). As shown in Figures 7(a) and 8 (a) and (b), the expression of PTPN2 mRNA and protein was both decreased in HG group compared to NC group and increased in HG+PTPN2 group compared to HG+Vehicle group. To evaluate osteogenesis capacity of RBMSCs, we detected ALP activity, and found that high glucose significantly reduced ALP activity, while the overexpression of PTPN2 could increase ALP activity compared to vehicle group (Figure 8(i)). We also quantified the expression of some osteogenic markers after 28 days of culture by qRT-PCR and Western blot. We found that high glucose significantly reduced mRNA and protein levels of OCN, OSX, and RUNX2, while the overexpression of PTPN2 could increase the levels of these markers compared to vehicle group (Figures 7(b) to (d) and 8(c) to (e)).

PTPN2 promoted the dephosphorylation of ERK in RBMSCs exposed to high glucose

To understand how osteogenic abilities of RBMSCs in high glucose were enhanced by PTPN2 overexpression,

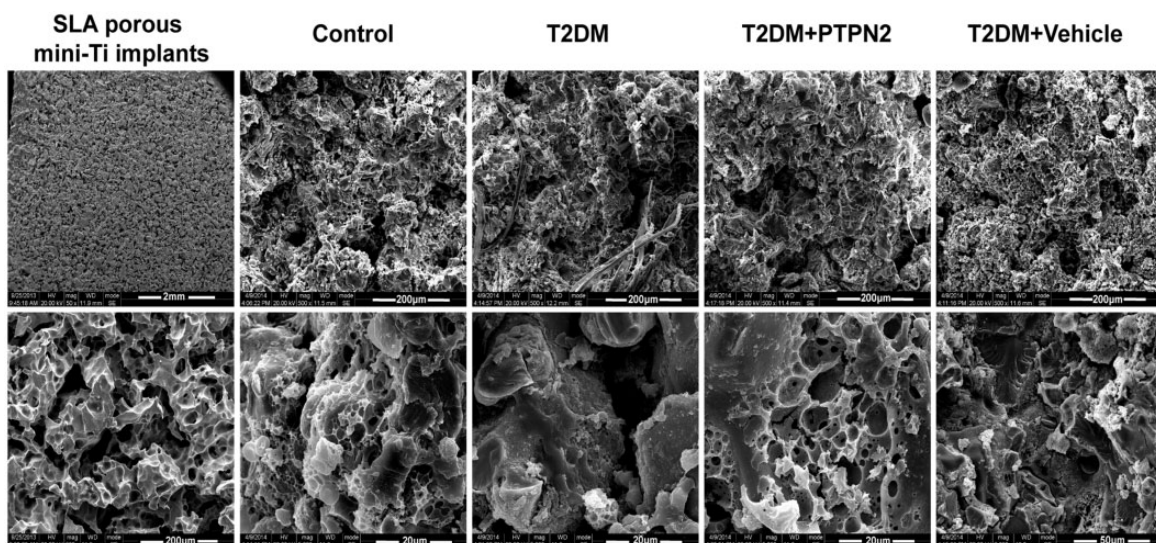


Figure 4. SEM images of SLA porous mini-Ti implants and peri-implant bone surfaces after three-month healing.

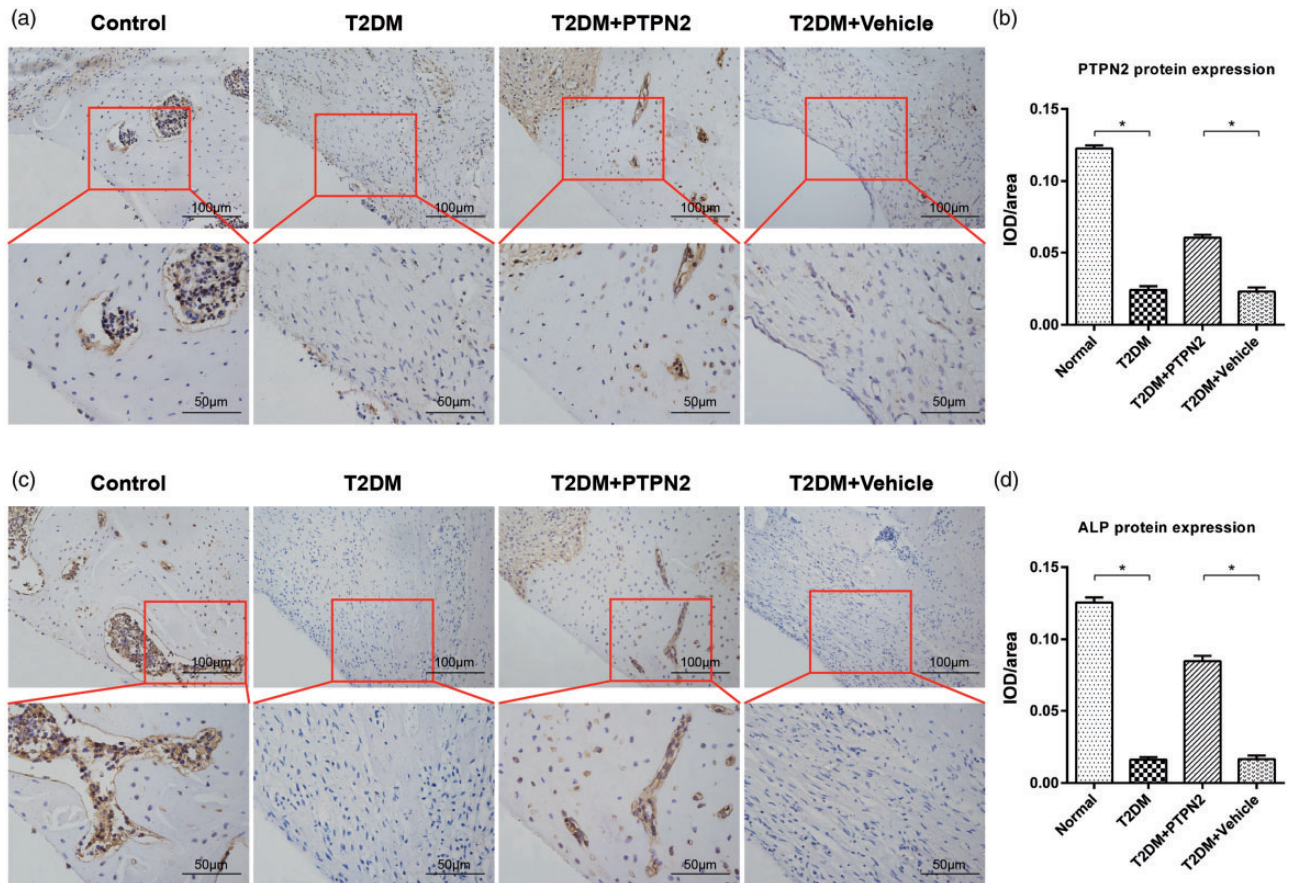


Figure 5. Expression of PTPN2 and ALP protein in the peri-implant bone area after three-month healing. Immunohistochemical images for (a) PTPN2 and (c) ALP, the magnifications of upper and lower images are 20 \times and 40 \times , respectively. Quantitative analysis of mean integral optical density (IOD) for PTPN2 (b) and ALP (d) were also presented. Data were presented as mean \pm SD, $n = 5$ specimens/group, $*P < 0.05$. (A color version of this figure is available in the online journal.)

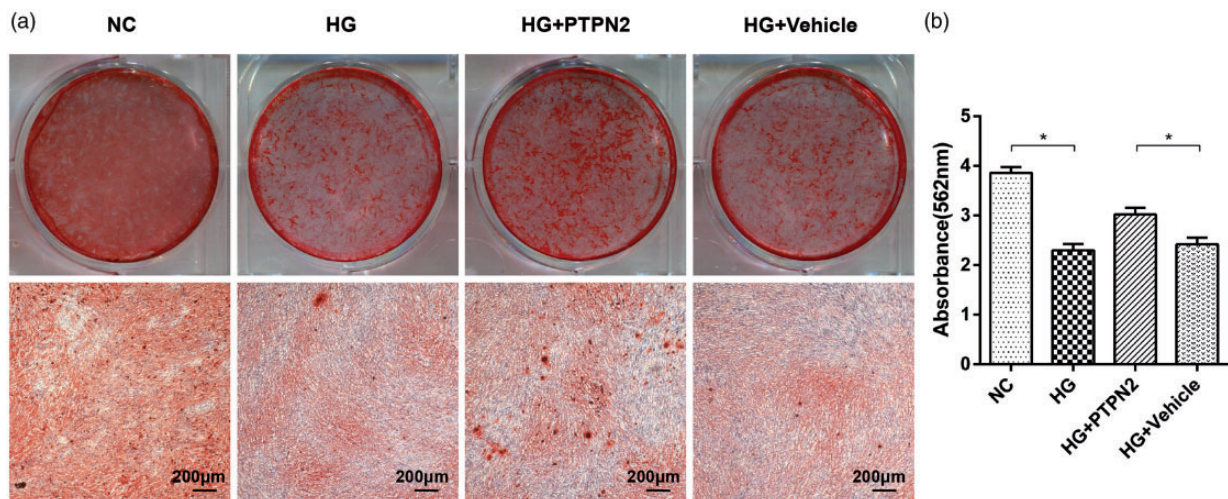


Figure 6. The overexpression of PTPN2 enhanced mineral deposition of RBMSCs after 28 days of osteogenic induction. (a) Representative photographs and low-lens pictures of Alizarin Red staining in different groups. (b) The concentration of calcium deposition was quantified by absorbance at 562 nm. Data were presented as mean \pm SD, $n = 5$ specimens/group, $*P < 0.05$. (A color version of this figure is available in the online journal.)

we detected the levels of ERK, p-ERK, JNK, p-JNK, p38, and p-p38. We found that the level of p-p38 increased in HG group compared to NC group but did not show significant differences between HG+PTPN2 group and

HG+Vehicle group (Figure 8(a) and (f)). The level of p-JNK did not show significant differences between HG group and NC group but decreased in HG+PTPN2 group compared to HG+Vehicle group (Figure 8(a) and (j)).

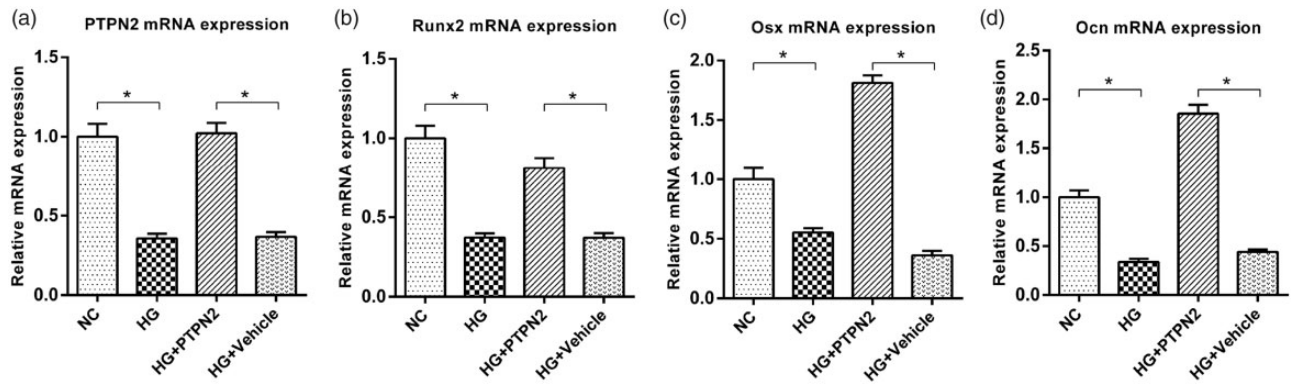


Figure 7. PTPN2 up-regulated the gene expression levels of Runx2, Osx, and Ocn of RBMSCs exposed to high glucose. (a) Gene expression levels of PTPN2 after 28 days of induction. (b) Gene expression levels of Runx2 after 28 days of induction. (c) Gene expression levels of Osx after 28 days of induction. (d) Gene expression levels of Ocn after 28 days of induction. Data were presented as mean \pm SD, $n = 5$ specimens/group, $*P < 0.05$.

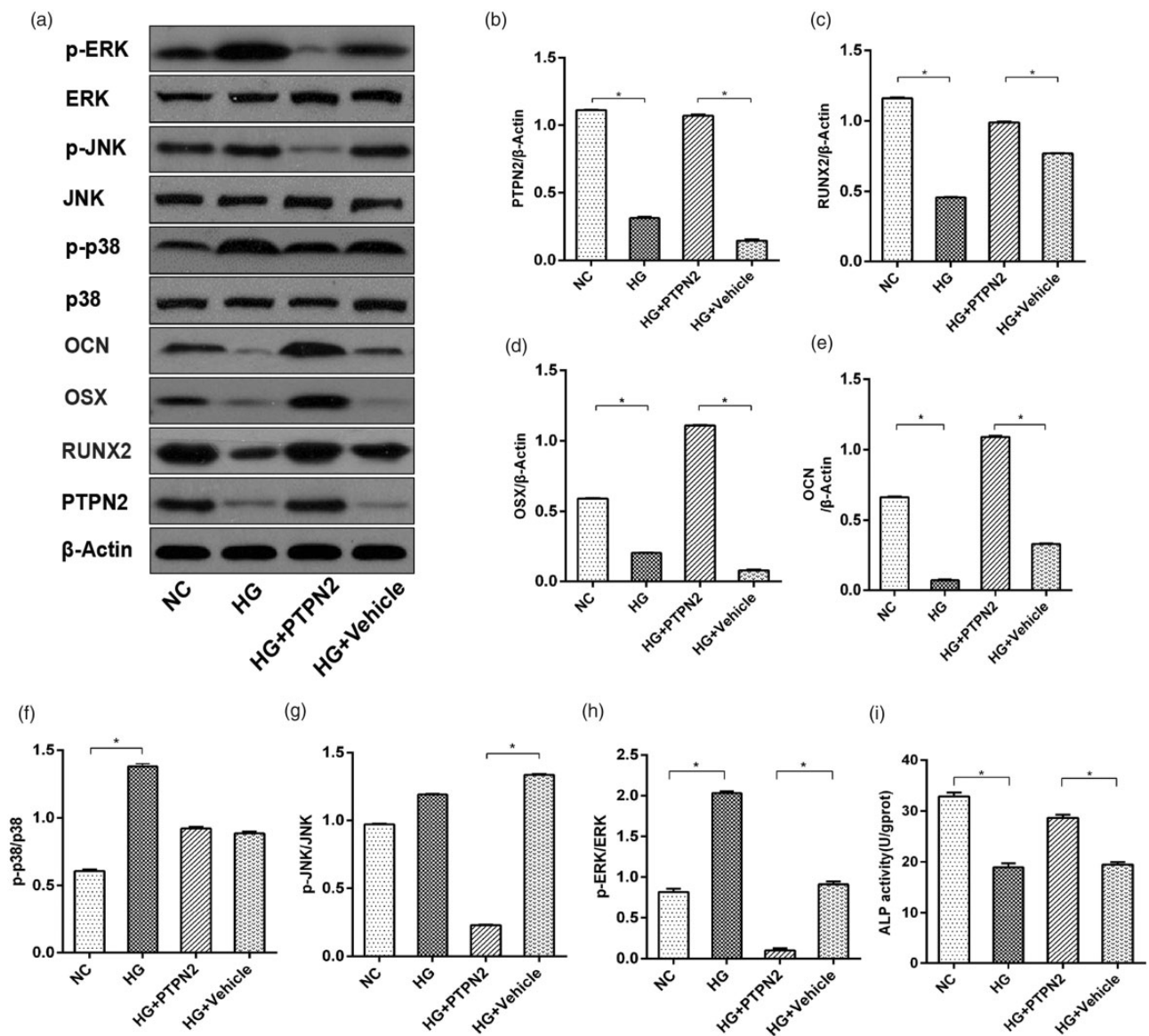


Figure 8. PTPN2 promoted osteogenesis of RBMSCs exposed to high glucose via inducing the dephosphorylation of ERK. (a) The protein levels of PTPN2, RUNX2, OSX, OCN, p38, p-p38, JNK, p-JNK, ERK, and p-ERK were assessed by Western blot analysis after 28 days of osteogenic induction. (b-h) The quantification analysis of protein levels. (i) Early osteogenic differentiation activity was detected by ALP activity at seven days. Data were presented as mean \pm SD, $n = 5$ specimens/group, $*P < 0.05$.

However, p-ERK increased in HG group compared to NC group and decreased in HG+PTPN2 group compared to HG+Vehicle group (Figure 8(a) and (h)). Collectively, these data suggest that PTPN2 selectively inhibits the activation of ERK branch of MAPK pathway in RBMSCs exposed to high glucose.

Discussion

In this study, we combined high-fat diet with low-dose STZ injection to induce rat model that resembles T2DM.^{21,22} We successfully established T2DM model with higher fasting glucose level and decreased body weight. In addition, PTPN2 local overexpression had no significant impact on the fasting blood glucose level and body weight in T2DM rats.

A growing body of evidence indicates that T2DM could impair implant osseointegration. The present study used a refined rat femur Ti implant model, which was designed referred to a previously published rat orthopedic implant protocol.¹⁷ In this study, we demonstrated a lower BIC% and OI% in T2DM group by histological evaluation and Micro-CT scanning. BIC% was used to describe the length percentage of direct bone-implant interface to total implant diameter in a two-dimensional figure, while OI% was used to describe the area proportion of direct bone-implant interface to total implant surface in three-dimensional structures. Furthermore, it was easier to pull the implant out in T2DM group which indicated the unsatisfactory biomechanical performance. Moreover, SEM analysis revealed impaired peri-implant bone microstructure in T2DM group. All these results confirmed the adverse effects of high glucose on osseointegration as reported in recent studies.²³

PTPN2 plays an important role in glucose metabolism. The pancreas-specific-PTPN2-knockout mice exhibited impaired glucose tolerance and attenuated glucose-stimulated insulin secretion (GSIS) with high-fat feeding.²⁴ It was reported that the deficiency of PTPN2 in the pancreas aggravated the apoptosis of β -cell induced by IL-1 β and IFN- γ .²⁵ On the other hand, high glucose can reduce the expression of PTPN2.²⁶ PTPN2 level in serum was much lower in T2DM patients than in healthy adults and negatively correlated with interleukin-6.²⁷ In this study, we found that the expression of PTPN2 was decreased in T2DM group around the implant *in vivo* and RBMSCs cultured in high glucose medium *in vitro*.

Considering the lethality of PTPN2-deficient mice caused by severe systemic inflammation²⁸ and the strong sensitivity to inflammatory stimuli in PTPN2 knockdown T cells or macrophages,^{29,30} the knockdown of PTPN2 in rats may cause inflammatory reaction and increase experimental variables. As a result, we chose local overexpression of PTPN2 to examine the effects of PTPN2 on osseointegration in T2DM rats. In this study, we observed positive effects of PTPN2 on implant osseointegration in T2DM rats. The implants in T2DM+PTPN2 group showed a higher BIC% and a better OI% compared with vehicle group. Furthermore, a 1.2-fold increase in the maximal pulling force and more well-organized bone microstructure was

observed after PTPN2 local overexpression. Moreover, PTPN2 increased the expression of ALP protein around the implant. Based on these results, we concluded that PTPN2 could improve bone microarchitecture and promote implant osseointegration in T2DM rats.

Furthermore, we supplemented the *in vivo* data with experiments *in vitro*. We successfully overexpressed PTPN2 in RBMSCs. ALP activity test, alizarin red staining, and Western blot analysis were used to evaluate osteogenic capacity of RBMSCs. ALP is an osteogenesis marker in early and middle stages which can hydrolyze phosphate to provide the necessary phosphoric acid for osteogenesis.³¹ We demonstrated that overexpression of PTPN2 could partly reverse ALP activity suppressed by high glucose. Alizarin red staining showed more mineralized nodules in cells of HG+PTPN2 group. OCN is produced by osteoblasts and is often used as a marker for bone formation. OSX is a novel zinc finger-containing transcription factor essential to osteoblast differentiation and bone formation.³² RUNX2 is a specific transcription factor that regulates osteogenic differentiation of mesenchymal stem cells.^{33,34} PCR and Western blot analysis showed overexpression of PTPN2 could overcome the suppression of the expression of these osteogenic mRNAs and proteins by high glucose. Taken together, our results indicated that PTPN2 could promote osteogenic differentiation of RBMSCs exposed to high glucose.

MAPKs are important components for the extracellular stimulus-mediated signal pathways which include ERK, JNK, and p38 MAPK.³⁵ ERK can be activated by extracellular responses, while p38 MAPK and JNK are activated through various stress stimulus, such as hyperglycemia.¹² Some articles find that ERK activation in osteoprogenitors is required for bone formation during skeletal development and homeostasis.³⁶ And ERK1/2 inhibition suppresses the osteogenic differentiation of human adipose-derived and dental pulp stem cells.^{37,38} However, the exact function of this signaling pathway is controversial. The activation of MAPKs by hyperglycemia plays a key role in mediating late complications. It was shown that increased p-p38 could lead to impaired osteogenesis of titanium implants in diabetes.¹³ Silva *et al.*³⁹ showed that gene expression of Alp of MSCs from STZ-induced diabetic rats was increased after incubating with specific inhibitors of the ERK (PD 98059), p38 (SB203580) for 6 h. Wang *et al.*⁴⁰ indicated that inhibition the ERK signaling pathways can induce osteoclastogenesis.

Our data showed the correlation between impaired osteogenic differentiation and increased levels of p-ERK and p-p38 in RBMSCs exposed to high glucose. Therefore, the inhibition of MAPK pathway would be an effective way to improve implant osseointegration in T2DM. Notably, PTPN2 can selectively modulate MAPK signaling in different conditions. For example, PTPN2 can modulate pancreatic β -cell apoptosis by regulating the phosphorylation of pro-apoptotic protein via Jun N-terminal Kinase 1(JNK1).^{25,41,42} PTPN2 overexpression inhibited TNF-induced activation of ERK and p38.¹⁴ In this study, we found that high glucose increased the phosphorylation of ERK and p38 but not JNK, while overexpression of

PTPN2 decreased the phosphorylation of ERK and JNK. These results suggest that PTPN2 may promote osteogenesis of RBMSCs in high glucose via inducing the dephosphorylation of p-ERK, but further studies are needed to provide direct evidence.

In summary, using both *in vivo* and *in vitro* approaches, we made important findings that PTPN2 promoted implant osseointegration in T2DM rats and enhanced osteogenesis of RBMSCs in high glucose medium. The positive effects of PTPN2 on osteogenesis are related to the dephosphorylation of ERK and the inhibition of MAPK/ERK pathway. PTPN2 may be a novel target for the therapy of impaired implant osseointegration in T2DM patients.

Authors' contributions: Zhang DJ designed the experiment, Wang YN listed the data systematically and wrote the manuscript; Jia TT performed the experiments *in vivo*; Zhang JJ performed the experiments *in vitro*; Lan J performed statistical analysis; Xu X guided all aspects of this study. All the authors listed have approved the manuscript and agree to publish.

DECLARATION OF CONFLICTING INTERESTS

The author(s) declared no potential conflicts of interest with respect to the research, authorship, and/or publication of this article.

FUNDING

This work was supported by grants from Fundamental Research Funds of Shandong University (2018GN024), Natural Science Foundation of Shandong Province (ZR2015HM065) and the Construction Engineering Special Fund of Taishan Scholars (TS201511106). Besides, the authors thank Dr. Yunmao Liao (Sichuan University) for his expertise with the implant preparation.

ORCID iD

Dongjiao Zhang  <https://orcid.org/0000-0003-2208-4922>

REFERENCES

- Javed F, Romanos GE. Impact of diabetes mellitus and glycemic control on the osseointegration of dental implants: a systematic literature review. *J Periodontol* 2009;**80**:1719–30
- Retzeppi M, Donos N. The effect of diabetes mellitus on osseous healing. *Clin Oral Implants Res* 2010;**21**:673–81
- Xiong Y, Zhang YX, Xin N, Yuan Y, Zhang Q, Gong P, Wu YY. 1,25-Dihydroxyvitamin D-3 promotes bone formation by promoting nuclear exclusion of the FoxO1 transcription factor in diabetic mice. *J Biol Chem* 2017;**292**:20270–80
- Hu X-F, Wang L, Lu Y-Z, Xiang G, Wu Z-X, Yan Y-B, Zhang Y, Zhao X, Zang Y, Shi L. Adiponectin improves the osteointegration of titanium implant under diabetic conditions by reversing mitochondrial dysfunction via the AMPK pathway *in vivo* and *in vitro*. *Acta Biomater* 2017;**61**:233–48
- Serrao CR, Bastos MF, Cruz DF, Malta FD, Vallim PC, Duarte PM. Role of metformin in reversing the negative impact of hyperglycemia on bone healing around implants inserted in type 2 diabetic rats. *Int J Oral Maxillofac Implants* 2017;**32**:547–54
- Ibarra-Sánchez Madj Simoncic PD, Nestel FR, Duplay P, Lapp WS, Tremblay ML. The T-cell protein tyrosine phosphatase. *Sem Immunol* 2000;**12**:379–86
- Smyth DJ, Plagnol V, Walker NM, Cooper JD, Downes K, Yang JHM, Howson JMM, Stevens H, McManus R, Wijmenga C. Shared and distinct genetic variants in type 1 diabetes and celiac disease. *N Engl J Med* 2008;**359**:2767–77
- Fukushima A, Loh K, Galic S, Fam B, Shields B, Wiede F, Tremblay ML, Watt MJ, Andrikopoulos S, Tiganis T. T-cell protein tyrosine phosphatase attenuates STAT3 and insulin signaling in the liver to regulate gluconeogenesis. *Diabetes* 2010;**59**:1906–14
- Li Y, Zhou HM, Wang F, Han L, Liu MH, Li YH, Wang ZH, Tang MX, Zhang W, Zhong M. Overexpression of PTPN2 in visceral adipose tissue ameliorated atherosclerosis via T cells polarization shift in diabetic apoe(-/-) mice. *Cell Physiol Biochem* 2018;**46**:118–32
- Zee T, Settembre C, Levine RL, Karsenty G. T-cell protein tyrosine phosphatase regulates bone resorption and whole-body insulin sensitivity through its expression in osteoblasts. *Mol Cell Biol* 2012;**32**:1080–8
- Chang LF, Karin M. Mammalian MAP kinase signalling cascades. *Nature* 2001;**410**:37–40
- Bhattacharjee N, Barma S, Konwar N, Dewanjee S, Manna P. Mechanistic insight of diabetic nephropathy and its pharmacotherapeutic targets: an update. *Eur J Pharmacol* 2016;**791**:8–24
- Wang L, Hu X, Ma X, Ma Z, Zhang Y, Lu Y, Li X, Lei W, Feng Y. Promotion of osteointegration under diabetic conditions by tantalum coating-based surface modification on 3-dimensional printed porous titanium implants. *Colloids Surf B Biointerfaces* 2016;**148**:440–52
- van Vliet C, Bukczynska PE, Puryer MA, Sadek CM, Shields BJ, Tremblay ML, Tiganis T. Selective regulation of tumor necrosis factor-induced ERK signaling by Src family kinases and the T cell protein tyrosine phosphatase. *Nat Immunol* 2005;**6**:253–60
- Hu Z, Ma C, Rong X, Zou S, Liu X. Immunomodulatory ECM-like microspheres for accelerated bone regeneration in diabetes mellitus. *ACS Appl Mater Interfaces* 2018;**10**:2377–90
- Fajardo RJ, Karim L, Calley VI, Bouxsein ML. A review of rodent models of type 2 diabetic skeletal fragility. *J Bone Miner Res* 2014;**29**:1025–40
- Li Y, Zou S, Wang D, Feng G, Bao C, Hu J. The effect of hydrofluoric acid treatment on titanium implant osseointegration in ovariectomized rats. *Biomaterials* 2010;**31**:3266–73
- Gao Y, Luo E, Hu J, Xue J, Zhu S, Li J. Effect of combined local treatment with zoledronic acid and basic fibroblast growth factor on implant fixation in ovariectomized rats. *Bone* 2009;**44**:225–32
- Zhou J, Jiang L, Long X, Fu C, Wang X, Wu X, Liu Z, Zhu F, Shi J, Li S. Bone-marrow-derived mesenchymal stem cells inhibit gastric aspiration lung injury and inflammation in rats. *J Cell Mol Med* 2016;**20**:1706–17
- Fang WJ, Wang CJ, He Y, Zhou YL, Peng XD, Liu SK. Resveratrol alleviates diabetic cardiomyopathy in rats by improving mitochondrial function through PGC-1alpha deacetylation. *Acta Pharmacol Sin* 2018;**39**:59–73
- Yin Y, Hao H, Cheng Y, Zang L, Liu J, Gao J, Xue J, Xie Z, Zhang Q, Han W. Human umbilical cord-derived mesenchymal stem cells direct macrophage polarization to alleviate pancreatic islets dysfunction in type 2 diabetic mice. *Cell Death Dis* 2018;**9**:760
- Xie Y, Chu A, Feng Y, Chen L, Shao Y, Luo Q, Deng X, Wu M, Shi X, Chen Y. MicroRNA-146a: a comprehensive indicator of inflammation and oxidative stress status induced in the brain of chronic T2DM rats. *Front Pharmacol* 2018;**9**:478
- King S, Klineberg I, Levinger I, Brennan-Speranza TC. The effect of hyperglycaemia on osseointegration: a review of animal models of diabetes mellitus and titanium implant placement. *Arch Osteoporos* 2016;**11**:29
- Xi Y, Liu S, Bettaieb A, Matsuo K, Matsuo I, Hosein E, Chahed S, Wiede F, Zhang S, Zhang ZY. Pancreatic T cell protein-tyrosine phosphatase deficiency affects beta cell function in mice. *Diabetologia* 2015;**58**:122–31
- Moore F, Colli ML, Cnop M, Esteve MI, Cardozo AK, Cunha DA, Bugliani M, Marchetti P, Eizirik DL. PTPN2, a candidate gene for type 1 diabetes, modulates interferon-gamma-induced pancreatic beta-cell apoptosis. *Diabetes* 2009;**58**:1283–91
- Simoncic PD, McGlade CJ, Tremblay ML. PTP1B and TC-PTP: novel roles in immune-cell signaling. *Can J Physiol Pharmacol* 2006;**84**:667–75

27. Zheng L, Zhang W, Li A, Liu Y, Yi B, Nakhoul F, Zhang H. PTPN2 downregulation is associated with albuminuria and vitamin D receptor deficiency in type 2 diabetes mellitus. *J Diabetes Res* 2018;**2018**:3984797
28. You-Ten KE, Muise ES, Itié A, Michaliszyn E, Wagner J, Jothy S, Lapp WS, Tremblay ML. Impaired bone marrow microenvironment and immune function in T cell protein tyrosine phosphatase-deficient mice. *J Exp Med* 1997;**186**:683–93
29. Heinonen KM, Nestel FP, Newell EW, Charette G, Seemayer TA, Tremblay ML, Lapp WS. T-cell protein tyrosine phosphatase deletion results in progressive systemic inflammatory disease. *Blood* 2004;**103**:3457–64
30. Spalinger MR, Kasper S, Chassard C, Raselli T, Frey-Wagner I, Gottier C, Lang S, Atrott K, Vavricka SR, Mair F. PTPN2 controls differentiation of CD4+ T cells and limits intestinal inflammation and intestinal dysbiosis. *Mucosal Immunol* 2014;**8**:918
31. Halling Linder C, Ek-Rylander B, Krumpel M, Norgård M, Narisawa S, Millán JL, Andersson G, Magnusson P. Bone alkaline phosphatase and tartrate-resistant acid phosphatase: potential co-regulators of bone mineralization. *Calcif Tissue Int* 2017;**101**:92–101
32. Ying C, Zhichao Z, Benoit DC, Kazuhisa N, Hui G, Xiaoping D, Shu-Fang J, Kleinerman ES. Osterix, a transcription factor for osteoblast differentiation, mediates antitumor activity in murine osteosarcoma. *Cancer Res* 2005;**65**:1124–8
33. Wei J, Shimazu J, Makinistoglu MP, Maurizi A, Kajimura D, Zong H, Takarada T, Lezaki T, Pessin JE, Hinoi E. Glucose uptake and Runx2 synergize to orchestrate osteoblast differentiation and bone formation. *Cell* 2015;**161**:1576–91 Jun 18;
34. Bruderer M, Richards RG, Alini M. Role and regulation of RUNX2 in osteogenesis. *Eur Cell Mater* 2014;**28**:269–86
35. Kiel C, Serrano L. Challenges ahead in signal transduction: MAPK as an example. *Curr Opin Biotechnol* 2012;**23**:305–14
36. Kim JM, Yang YS, Park KH. The ERK MAPK pathway is essential for skeletal development and homeostasis. *Int J Mol Sci* 2019;**20**:1803
37. Quarto N, Senarath-Yapa K, Renda A, Longaker MT. TWIST1 silencing enhances in vitro and in vivo osteogenic differentiation of human adipose-derived stem cells by triggering activation of BMP-ERK/FGF signaling and TAZ upregulation. *Stem Cells* 2015;**33**:833–47
38. Song F, Sun H, Huang L, Fu D, Huang C. The role of Pannexin3-modified human dental pulp-derived mesenchymal stromal cells in repairing rat cranial critical-sized bone defects. *Cell Physiol Biochem* 2017;**44**:2174–88
39. Silva JC, Sampaio P, Fernandes MH, Gomes PS. The osteogenic priming of mesenchymal stem cells is impaired in experimental diabetes. *J Cell Biochem* 2015;**116**:1658–67
40. Wang C, Xiao F, Qu X, Zhai Z, Hu G, Chen X, Zhang X. Sitagliptin, an anti-diabetic drug, suppresses estrogen deficiency-induced osteoporosis in vivo and inhibits RANKL-Induced osteoclast formation and bone resorption in vitro. *Front Pharmacol* 2017;**8**:407
41. Santin I, Eizirik DL. Candidate genes for type 1 diabetes modulate pancreatic islet inflammation and beta-cell apoptosis. *Diabetes Obes Metab* 2013;**15**: 71–81
42. Santin I, Moore F, Colli ML, Gurzov EN, Marselli L, Marchetti P, Eizirik DL. PTPN2, a candidate gene for type 1 diabetes, modulates pancreatic β -cell apoptosis via regulation of the BH3-only protein Bim. *Diabetes* 2011;**60**:3279–88

(Received July 17, 2019, Accepted September 27, 2019)